

On reducible nonlinear time-delayed stochastic systems: fluctuation-dissipation relations, transitions to bistability, and secondary transitions to non-stationarity

**K. Patanarapeelert¹, T.D. Frank², R. Friedrich², and
I.M. Tang³**

¹ Faculty of Science, Department of Mathematics, Mahidol University, Rama VI Road, Bangkok 10400, Thailand

² Institute for Theoretical Physics, University of Münster, Wilhelm-Klemm-Str. 9, 48149 Münster, Germany

³ Faculty of Science, Department of Physics, Mahidol University, Rama VI Road, Bangkok 10400, Thailand

Abstract.

We show under which conditions, nonlinear time-delayed dynamical systems with multiplicative noise sources can be transformed into linear time-delayed systems with additive noise sources. We show that for such reducible systems, analytical expressions for stationary distributions can be obtained. We demonstrate that fluctuation-dissipation relations of reducible systems become trivial and we show that reducible systems may exhibit delay- and noise-induced transitions to bistability and secondary transitions to non-stationarity. Our general findings are exemplified for three models: a Gompertz model, a Hongler model and a model involving a $1 - x^2$ noise amplitude.

Submitted to: *J. Phys. A: Math. Gen.*

PACS numbers: 05.40.-a, 02.30.Ks, 02.50.Ey

1. Introduction

In a variety of applications, stochastic delay differential equations (SDDEs) portray real-life and artificial systems involving memory effects (time delays) coupled to spontaneous fluctuations (noise). Time delays play important roles in laser physics [1, 2, 3, 4, 5, 6, 7], chaos control [8], and engineering sciences [9, 10, 11, 12]. Time delays are typically involved in biological systems [13], in particular, in motor control systems [14, 15, 16, 17, 18, 19], neural network systems [20, 21, 22, 23, 24, 25], and ecological systems [26]. Noise can be observed as thermal noise [27] and multiplicative noise [28]. For example, we are dealing with multiplicative noise when the fertility parameter of the logistic model for population growth fluctuates around a mean value [29]. Moreover, there is evidence that balancing movements [17] and the pupil dynamics [15, 30, 31] crucially depend on the impact of multiplicative noise.

Time delays and noise can affect the dynamics of systems in different ways. In the absence of noise, stable systems can become unstable when time delays exceed certain critical values. In the absence of time delays, multiplicative noise can induce transition phenomena known as noise-induced transitions [28]. In systems exhibiting time delays and multiplicative noise, both phenomena can occur and the critical control parameters, namely, the critical delays and the critical noise amplitudes, will depend on each other. Therefore, a central aim is to combine analytical tools derived for time delayed systems [9, 32, 33] and stochastic systems with multiplicative noise [28] and to study the solutions of delay differential equations that involve multiplicative noise. However, in the context of SDDEs, we are still far away from an analytical approach. For instance, the derivation of exact stationary distribution is still an unsolved problem. For systems without time delays variable transformations that map nonlinear systems with multiplicative noise sources to linear systems with additive noise sources have become important solution methods. In particular, a general condition for which nonlinear systems with multiplicative noise are reducible and can be transformed into linear additive noise systems has been shown in [28, 29, 34]. Therefore, the aim is to generalize

this variable transformation method to time-delayed multiplicative noise systems. In particular, it would be helpful to derive the condition under which a nonlinear SDDE can be transformed into a linear additive noise SDDE and can be solved analytically.

The paper is organized as follows. In Sec. 2 we derive the condition for which a nonlinear SDDE can be transformed into a linear one. We show explicitly that if this condition holds, then the corresponding delay Fokker-Planck equation (DFPE) becomes a linear additive noise DFPE as well. The stationary distributions of systems satisfying this condition are obtained. Moreover, in Sec. 3 a dissipation-fluctuation relation is discussed for reducible systems. For the applications we give three example models (see Sec. 4): the Gompertz model, the Hongler model and a $1 - x^2$ noise model. Finally, we give conclusions and some discussions in Sec. 5.

2. Variable transformations of nonlinear systems to a linear ones

2.1. Transformation of nonlinear stochastic delay differential equations to linear ones

In this section, we show that the Stratonovich SDDE

$$\frac{d}{dt}X(t) = h(X(t), X(t - \tau)) + g(X(t))\Gamma(t), \quad (1)$$

where $\Gamma(t)$ is assumed to be a Gaussian random force with zero mean and obeys $\langle \Gamma(t)\Gamma(t') \rangle = \delta(t - t')$, can be transformed into the linear SDDE

$$\frac{d}{dt}Y(t) = -aY(t) - bY(t - \tau) + \sqrt{Q}\Gamma(t), \quad (2)$$

under the condition

$$g(X)d[h(X, X_\tau)] = -ag(X)dX - b\frac{g^2(X)}{g(X_\tau)}dX_\tau + h(X, X_\tau)d[g(X)], \quad (3)$$

where X denotes $X(t)$ and $X_\tau = X(t - \tau)$. In order to verify this condition, we assume that there is a function f such that $Y = f(X)$ is an invertible variable transformation. That is, $X = f^{-1}(Y)$ is well defined. It follows that

$$\frac{d}{dt}Y(t) = \frac{df(X)}{dX}h(X, X_\tau) + \frac{df(X)}{dX}g(X)\Gamma(t). \quad (4)$$

Since the new variable Y satisfies the linear SDDE (2), one obtains

$$\underbrace{-af(X) - bf(X_\tau)}_A + \underbrace{\sqrt{Q}\Gamma(t)}_B = \underbrace{\frac{df(X)}{dX}h(X, X_\tau)}_A + \underbrace{\frac{df(X)}{dX}g(X)\Gamma(t)}_B.$$

Comparing the A and B terms, we find

$$f(X) = \int^X \frac{\sqrt{Q}}{g(X')} dX' + C, \quad (5)$$

where C is constant, and

$$h(X, X_\tau) = \frac{g(X)}{\sqrt{Q}} \{-af(X) - bf(X_\tau)\}. \quad (6)$$

The total differential of the drift term can be expressed as

$$\begin{aligned} d[h(X, X_\tau)] = & -adX - b\frac{g(X)}{g(X_\tau)}dX_\tau \\ & - \frac{1}{\sqrt{Q}}\frac{dg(X)}{dX}\{af(X) + bf(X_\tau)\}dX. \end{aligned} \quad (7)$$

Multiplying Eq. (7) with $g(X)$ and collecting terms dX and dX_τ , we get

$$g(X)\frac{\partial}{\partial X}h(X, X_\tau) = -ag(X) + h(X, X_\tau)\frac{dg(X)}{dX} \quad (8)$$

and

$$g(X)\frac{\partial}{\partial X_\tau}h(X, X_\tau) = -b\frac{g^2(X)}{g(X_\tau)}. \quad (9)$$

Adding Eqs. (8) and (9) together, we recover Eq. (3). For nonlinear systems without delay we put $\tau = 0$ in Eq. (8), then Eq. (8) is the condition derived in previous works [29, 34].

2.2. Transformation of nonlinear delay Fokker-Planck equations to linear ones

Next, we consider the DFPE

$$\begin{aligned} \frac{\partial}{\partial t}P(x, t) = & -\frac{\partial}{\partial x}\int h(x, x_\tau)P(x, t; x_\tau, t - \tau)dx_\tau \\ & + \frac{1}{2}\frac{\partial}{\partial x}g(x)\frac{\partial}{\partial x}g(x)P(x, t), \end{aligned} \quad (10)$$

associated with the Stratonovich SDDE (1). As shown in Sec. 2.1, under condition (3) the DFPE (10) can be transformed into the linear DFPE

$$\frac{\partial}{\partial t}P(y, t) = \frac{\partial}{\partial y}\int (ay + by_\tau)P(y, t; y_\tau, t - \tau)dy_\tau + \frac{Q}{2}\frac{\partial^2}{\partial y^2}P(y, t), \quad (11)$$

using the transformation $y = f(x)$. Indeed, we will derive next Eq. (11) directly from Eq. (10). To this end, we begin with providing the relation between the probability densities $P(x, t)$ and $P(y, t)$. Suppose that $P(x, t)$ is a probability density of the random variable X defined by $P(x, t) = \langle \delta(x - X) \rangle$ and $P(y, t)$ is a probability density of the random variable Y defined by $P(y, t) = \langle \delta(y - Y) \rangle$. Using the variable transformation $Y = f(X)$, we can write [35]

$$P(x, t) = P(y, t) \left| \frac{dy}{dx} \right|. \quad (12)$$

Extending this relation to multiple variables, it follows that the joint probability densities $P(x, t; x_\tau, t - \tau)$ and $P(y, t; y_\tau, t - \tau)$ satisfy

$$P(x, t; x_\tau, t - \tau) dx_\tau = P(y, t; y_\tau, t - \tau) \left| \frac{dy}{dx} \right| dy_\tau. \quad (13)$$

It follows from Eq. (10) that the derivative with respect to t can be written in terms of the derivative of y with respect to t like $\partial P(x, t)/\partial t = f'(x)P(y, t)$. By inserting Eq. (6) and Eq. (13) into the DFPE (10), we obtain

$$\begin{aligned} & \left(\frac{dy}{dx} \right) \frac{\partial}{\partial t} P(y, t) = \\ & - \left(\frac{dy}{dx} \right) \frac{\partial}{\partial y} \int \frac{g(x)}{\sqrt{Q}} \{ -af(x) - bf(x_\tau) \} P(y, t; y_\tau, t - \tau) \left| \frac{dy}{dx} \right| dy_\tau \\ & + \frac{1}{2} \left(\frac{dy}{dx} \right) \frac{\partial}{\partial y} g(x) \left(\frac{dy}{dx} \right) \frac{\partial}{\partial y} g(x) P(y, t) \left| \frac{dy}{dx} \right|. \end{aligned} \quad (14)$$

Using $g(x)f'(x) = \sqrt{Q}$, we obtain the linear DFPE (11) corresponding to the linear SDDE (2).

2.3. Linear SDDE revisited

Since all nonlinear problems satisfying condition (3) can be mapped to the linear equation (2), it is worth while to review some basic properties of Eq. (2).

2.3.1. Case $Q = 0$

Let λ be an eigenvalue of the deterministic delay differential equation $\dot{Y} = -aY - bY_\tau$ related to Eq. (2). The fixed point is $Y_{\text{st}} = 0$. In order to determine the

stability of this fixed point we note that the characteristic equation of the deterministic delay differential equation is given by

$$\lambda + a + be^{-\lambda\tau} = 0. \quad (15)$$

First of all, we have a stationary bifurcation at the line $a = -b$ with $(a, b) = (-1/\tau, 1/\tau) \cdots (\infty, \infty)$ (see Fig. 1). Second, if $b \geq |a|$ holds, then an oscillatory (Hopf) bifurcation can occur at a critical delay τ_c given by

$$\tau_c = \frac{1}{\sqrt{b^2 - a^2}} \arccos\left(-\frac{a}{b}\right). \quad (16)$$

For any $\tau < \tau_c$ the boundary of the stable region in the parameter space (a, b) can be determined by the parametric equations [32, 33]

$$\begin{aligned} b(\omega) &= \frac{\omega}{\sin(\omega\tau)}, \\ a(\omega) &= -\omega \cot(\omega\tau), \end{aligned} \quad (17)$$

where $\omega = \sqrt{b^2 - a^2}$. Note that the parametric bifurcation line includes the point $(a, b) = (-1/\tau, 1/\tau)$ for $\omega \rightarrow 0$ (i.e. for $b \rightarrow -a > 0$) such that the oscillatory (parametric) bifurcation line and the stationary (straight) bifurcation line merge at $(a, b) = (-1/\tau, 1/\tau)$. Note also that on the line $b = a > 0$ we have $\tau_c \rightarrow \infty$, which implies that for this condition the fixed point $Y_{\text{st}} = 0$ is stable for every $\tau \geq 0$. Furthermore, if $a > |b|$ holds, then the fixed point $Y_{\text{st}} = 0$ is stable again for every $\tau \geq 0$. Therefore, the domain of stability is composed of the region $b \geq |a|$ with $\tau < \tau_c$ and $a \neq -b$ and of the region $a > |b|$ (see also Fig. 1 again).

Insert Figure 1 about here

2.3.2. Case $Q > 0$

Due to the fact that the system is linear and the noise $\Gamma(t)$ is a Langevin force, one can show that the existence of the stationary solution of Eq. (2) depends on the domain of stability of the fixed point Y_{st} of its deterministic counterpart. Namely, the stationary distribution of Eq. (2) exists if $b > |a|$ with $\tau < \tau_c$ and $a > |b|$. In this case,

the stationary distribution is the Gaussian distribution [36, 37, 38, 39]

$$P_{\text{st}}(y) = \frac{1}{\sqrt{2\pi K(\tau)}} \exp \left\{ -\frac{y^2}{2K(\tau)} \right\}. \quad (18)$$

The variance $K(\tau)$ can be expressed as

$$K(\tau) = \begin{cases} \frac{Q}{2} \left(\frac{1 + b\omega^{-1} \sin(\omega\tau)}{a + b \cos(\omega\tau)} \right), & b > |a|, \quad \tau < \tau_c \\ \frac{Q}{2} \left(\frac{1 + b\omega^{-1} \sinh(\omega\tau)}{a + b \cosh(\omega\tau)} \right), & a > |b| \\ \frac{Q}{4a} (1 + a\tau), & a = b \end{cases} \quad (19)$$

For $b > |a|$ at the oscillatory (Hopf) bifurcation, variance of the stationary distribution becomes infinity. In particular, at the critical delay, we find

$$b \cos(\omega\tau_c) + a = 0,$$

which yields,

$$K(\tau_c) = \frac{Q}{2} \left[\frac{1 + b\omega^{-1} \sin(\omega\tau_c)}{a + b \cos(\omega\tau_c)} \right] \rightarrow \infty.$$

In addition, at the stationary bifurcation line, we also find that the variance becomes infinity at $b = -a$. To demonstrate this, we can consider the limiting cases $a \rightarrow -b$ and $b \rightarrow -a$. Both cases lead to $K(\tau) \rightarrow \infty$ irrespective of τ . Finally note that $K(\tau)$ is a monotonic function with respect to τ . For $b > |a|$ we have (see also [39])

$$\frac{d}{d\tau} K(\tau) = \frac{b^2 Q}{2} \left(\frac{1 + \cos(\omega\tau + \varphi_1)}{[a + b \cos(\omega\tau)]^2} \right) > 0, \quad (20)$$

where φ_1 denotes a phase that depends on the parameters a and b . As indicated in Eq. (20) the variance increases monotonically as a function of τ (both for $a > 0$ and $a < 0$).

For $a > |b|$ we have

$$\frac{d}{d\tau} K(\tau) = \frac{bQ}{2} \left(\frac{a \cosh(\omega\tau) - \omega \sinh(\omega\tau) + b}{[a + b \cosh(\omega\tau)]^2} \right). \quad (21)$$

From $\omega < a$ it follows that $a \cosh(\omega\tau) - \omega \sinh(\omega\tau) > 0$ holds for $\tau \geq 0$, which in turn gives us the relation $a \cosh(\omega\tau) - \omega \sinh(\omega\tau) = |b| \cosh(\omega\tau + \varphi_2)$, where $\varphi_2 = \varphi_2(a, b) < 0$ denotes a phase variable again. Eq. (21) can then be transformed into

$$\frac{d}{d\tau} K(\tau) = \frac{bQ}{2} \left(\frac{|b| \cosh(\omega\tau + \varphi_2) + b}{[a + b \cosh(\omega\tau)]^2} \right). \quad (22)$$

For $b > 0$ we see from Eq. (22) that the variance increases monotonically as a function of τ . In contrast, for $b < 0$ the expression $|b| \cosh(\omega\tau + \varphi_2) + b$ is semi-positive for all τ (in fact it is strictly positive for all τ except for $\tau^* = -\varphi_2/\omega$). Consequently, for $b < 0$ the variance (22) decreases monotonically with τ .

2.4. Stationary distributions of reducible systems

Again, we consider the nonlinear SDDE

$$\frac{d}{dt}X(t) = h(X(t), X(t - \tau); \vec{\alpha}) + g(X(t); \vec{\beta})\Gamma(t), \quad (23)$$

with additional parameters $\vec{\alpha} = (\alpha_1, \alpha_2, \dots)$ and $\vec{\beta} = (\beta_1, \beta_2, \dots)$. Using $Y = f(X)$, the system (23) can be transformed into the linear SDDE (2) and the parameter space $(\vec{\alpha}, \vec{\beta})$ can be mapped to the parameter space (a, b) by $a = a(\vec{\alpha}, \vec{\beta})$ and $b = b(\vec{\alpha}, \vec{\beta})$. By inverse mapping, we can determine the parameter conditions for the existence of stationary distributions of Eq. (23) in terms of the parameters $\vec{\alpha}$ and $\vec{\beta}$. From Eq. (12) and Eq. (18) it follows that the stationary distribution of the nonlinear SDDE (23) is given by

$$P_{\text{st}}(x) = \frac{1}{\sqrt{2\pi K(\tau)}} \exp \left\{ -\frac{[f(x)]^2}{2K(\tau)} \right\} |f'(x)|, \quad (24)$$

with $K(\tau) = K(\tau; a(\vec{\alpha}, \vec{\beta}), b(\vec{\alpha}, \vec{\beta}))$.

3. Generalized fluctuation-dissipation theorem

3.1. Systems without time delay

We first consider systems without delay for which the drift term is in form $h(X(t))$ and introduce the total fluctuating force $\xi(X, t) = g(X)\Gamma(t)$. Thus, the stochastic differential equation can be written as

$$\frac{d}{dt}X(t) = h(X(t)) + \xi(X(t), t). \quad (25)$$

Assume that the probability current vanishes in the stationary case. Then, the following balance equation holds

$$\langle h \rangle = -\langle \xi \rangle. \quad (26)$$

In the meteorological literature, this balance equation is called *generalized dissipation-fluctuation theorem* [40]. We would like to point out that this balance relation should not be confused with dissipation-fluctuation theorems of the Green-Kubo theory [41].

3.2. Systems with time delay and time-delayed reducible systems

It is clear that the relation (26) holds also for systems with time delays, that is, for systems satisfying Eq. (1). In addition, for reducible systems with time delays we have the following two properties:

(a) For the variable transformation $X \rightarrow Y$ the multiplicative noise source is transformed into additive noise and the nonlinear drift force becomes linear. In particular, the drift and diffusion terms are transformed into $h_Y = -(aY + bY_\tau)$ and $\xi_Y = \sqrt{Q}\Gamma(t)$ and their averages satisfy

$$\langle h_Y \rangle = 0, \quad \langle \xi_Y \rangle = 0. \quad (27)$$

For reducible time-delayed systems a "stronger" version of the fluctuation-dissipation relation (26) holds which is given by (27).

(b) In some cases analytical expressions for the averages $\langle h \rangle$ and $\langle \xi \rangle$, respectively, can be derived by means of the transformation to the linear system. Comparing the Fokker-Planck description in the previous section with the Langevin description (see Eq. (1)), we see that

$$\langle \xi \rangle_{\text{st}} = -\frac{1}{2} \int_{\Omega} g \frac{\partial}{\partial x} [g(x) P_{\text{st}}(x)] dx,$$

(where we assume again that the probability current vanishes such that surface terms arising due to partial integration can be neglected). This implies

$$\begin{aligned} \langle h \rangle_{\text{st}} = -\langle \xi \rangle_{\text{st}} &= \frac{1}{2} \int_{-\infty}^{\infty} g(f^{-1}(y)) \frac{d}{dy} P_{\text{st}}(y) dy, \\ &= -\frac{1}{2} \int_{-\infty}^{\infty} P_{\text{st}}(y) \frac{d}{dy} g(f^{-1}(y)) dy. \end{aligned} \quad (28)$$

Here, we assume that the surface term $g(f^{-1}(y))P_{\text{st}}(y)$ vanishes for $y \rightarrow \pm\infty$. For examples see Sec. 4.2.

4. Examples

4.1. Numerics

In the following examples, we will present both analytical and numerical results. We obtained the numerical results from the relevant SDDEs. To this end, the Stratonovich SDDEs were first transformed into the corresponding Itô SDDEs. That is, the SDDEs of the form (1) were transformed into

$$\frac{d}{dt}X(t) = h(X(t), X(t - \tau)) + \frac{1}{2}g(X(t))\frac{dg(X(t))}{dX} + g(X(t))\Gamma(t). \quad (29)$$

The Itô SDDEs were then solved numerically by means of an stochastic Euler forward algorithm [35] that is known to hold also for time-delayed equations [42]. Accordingly, Eq. (29) was solved on a time interval that was divided into finite steps of Δt . The random variable $X_n = X(t_n)$ for the discrete time points $t_n = n\Delta t$ with $n = 0, 1, 2, \dots$, were computed from

$$X_{n+1} = X_n + \Delta t \left\{ h(X_n, X_{n-m}) + \frac{1}{2}g(X_n)\frac{dg(X_n)}{dX_n} \right\} + \sqrt{\Delta t}g(X_n)w_n, \quad (30)$$

where $X_{n-m} = X(t_{n-m})$ denotes the retarded random variable with a discrete time delay of $\tau = m\Delta t$. In Eq. (30) w_n is the Gaussian random generator with $\langle w_n \rangle = 0$ and $\langle w_n w_{n'} \rangle = \delta_{nn'}$ (obtained from a Box-Muller algorithm). The initial condition in all simulations was $X_n = x_0$ for $n \in [-m, 0]$. For every realization we iterated Eq. (30) T times with T sufficiently large such that the final random value X_T represented the stationary case. Using this procedure, for a given SDDE we computed N realizations of X_T and derived from this set of realizations the stationary probability density of the SDDE.

4.2. Gompertz model

We first consider the SDDE given by

$$\frac{d}{dt}X = -\tilde{a}X \ln(X/c) - \tilde{b}X \ln(X(t-\tau)/c) + \sqrt{\tilde{Q}}X\Gamma(t), \quad (31)$$

with $c > 0$ and $\tilde{a}, \tilde{b} \in \mathbb{R}$, $X \in [0, \infty)$; $\vec{a} = (\tilde{a}, \tilde{b}, c)$, $\beta = \tilde{Q}$. Using the variable transformation $Y = \ln(X/c)$, we obtain Eq. (2) with $a = \tilde{a}$, $b = \tilde{b}$ and $Q = \tilde{Q}$. Hence, we can find that if the relation $\tilde{b} \geq |\tilde{a}|$ with $\tilde{a} \neq -\tilde{b}$ and $\tau < \tau_c = (\tilde{b}^2 - \tilde{a}^2)^{-1/2} \arccos(-\tilde{a}/\tilde{b})$ holds or if the relation $\tilde{a} > |\tilde{b}|$ holds, then the stationary distribution of the Gompertz model (31) exists. As a result of the mapping $Y = \ln(X/c)$ and Eq. (24), the stationary distribution can be expressed as

$$P_{\text{st}}(x) = \frac{1}{x} \frac{1}{\sqrt{2\pi K(\tau)}} \exp \left\{ - \left[\ln \frac{x}{c} \right]^2 \frac{1}{2K(\tau)} \right\}, \quad (32)$$

with $K(\tau)$ defined by Eq. (19). Eq. (32) includes distributions obtained in previous studies as special cases. For instance, in the case $\tilde{a} = 0$, the stationary distribution of Eq. (31) is given by Eq. (32) with

$$K(\tau) = \frac{Q}{2} \left(\frac{1 + \sin(b\tau)}{b \cos(b\tau)} \right), \quad (33)$$

which is equivalent to the distributions derived in [43]. In the case $\tilde{b} = 0$, from Eq. (32) we have

$$P_{\text{st}}(x) = \frac{1}{x} \sqrt{\frac{\tilde{a}}{\pi \tilde{Q}}} \exp \left\{ - \left[\ln \frac{x}{c} \right]^2 \frac{\tilde{a}}{\tilde{Q}} \right\}, \quad (34)$$

which recover the result in [44]. Fig. 2 shows the stationary probability densities of the Gompertz model (31) given by Eq. (32) for different parameters between a and b .

Insert Figure 2 about here

Next, we will consider the balance of drift and diffusion terms for the Gompertz model (31). In Sec. 3, we showed that the average drift term can be calculated analytically by utilization of variable transformation. From Eq. (28) we find that

$$\langle h \rangle = -\frac{c\sqrt{\tilde{Q}}}{2} \int_{-\infty}^{\infty} e^y \left(\frac{dP_{\text{st}}(y)}{dy} \right) dy,$$

which reads explicitly

$$\langle h \rangle = \frac{c\sqrt{\tilde{Q}}}{2} e^{(K(\tau)/2)}. \quad (35)$$

In Fig. 3 we show that for $\tilde{a} > |\tilde{b}|$ the average drift term $\langle h \rangle$ given by Eq. (35) approaches to a constant as the delay tends to infinity.

Insert Figure 3 about here

4.3. Noise-induced transition to bistability

In this section we study the impact of time delays on noise-induced transitions. To this end, we will consider two models: (i) a time-delayed Hongler model and (ii) a model involving a noise amplitude of the form $1 - x^2$. Note that the Hongler model [28, 45, 46] as well as models with $1 - x^2$ amplitudes [47] play important roles for our understanding of noise-induced transitions because they can be solved analytically.

4.3.1. Hongler model

We consider first the Hongler model defined by

$$\frac{d}{dt}X(t) = -\tilde{a} \tanh(cx) - \tilde{b} \frac{\sinh(cx_\tau)}{\cosh(cx)} + \frac{\sqrt{\tilde{Q}}}{\cosh(cx)} \Gamma(t), \quad (36)$$

where $c > 0$ and $\tilde{a}, \tilde{b} \in \mathbb{R}$, $X \in \mathbb{R}$. Eq. (5) gives us the transformation $Y = \sinh(cx)/c$ which transforms Eq. (36) into Eq. (2) with $a = \tilde{a}, b = \tilde{b}, Q = \tilde{Q}$. Consequently, with respect to the parameter space (\tilde{a}, \tilde{b}) the stationary distribution of Hongler model (36) exists if the condition $\tilde{b} \geq |\tilde{a}|$ with $\tilde{a} \neq -\tilde{b}$ and $\tau < \tau_c = (\tilde{b}^2 - \tilde{a}^2)^{-1/2} \arccos(-\tilde{a}/\tilde{b})$ holds or if the condition $\tilde{a} > |\tilde{b}|$ is satisfied. With the help of Eq. (24), the stationary distribution of the Hongler model (34) is given by

$$P_{\text{st}}(x) = \frac{1}{\sqrt{2\pi K(\tau)}} \exp \left\{ -\frac{\sinh^2(cx)}{2c^2 K(\tau)} \right\} \cosh(cx), \quad (37)$$

with $K(\tau)$ given by Eq. (19). For $\tilde{a} = 0$ the function $K(\tau)$ reduces to Eq. (33) and we obtain the stationary distribution (37) with Eq. (33) which has been previously derived in [48].

Insert Figure 4 about here

Next, we will consider the delay and noise induced transition to bistability. By using the generalized stationary distribution Eq. (37), it was shown in a previous study

[48] the transition occurs at

$$K(\tau) = \frac{1}{c^2}. \quad (38)$$

In contrast to the aforementioned previous study for which $\tilde{a} = 0$ holds, we need to distinguish now between three cases: $\tilde{b} > |\tilde{a}|$, $\tilde{a} = \tilde{b}$, $\tilde{a} > |\tilde{b}|$. Let us discuss delay- and noise-induced transitions for these three cases in terms of the $\tau - Q$ plane, see Fig. 5. In the case $\tilde{b} > |\tilde{a}|$ (see Fig. 5(a)), increasing delay or noise strength can result in the stationary distribution (unimodal distribution) becoming a bimodal distribution (see also Fig. 4). In addition, there is a critical delay τ_c for which the stationary distribution does not exist. That is, the Hongler model exhibits a nonstationary state as the delay is increased over the critical delay. In the cases $\tilde{b} = \tilde{a}$ and $\tilde{a} > |\tilde{b}|$ the stationary distribution exists for all time delays $\tau \geq 0$. In the case $\tilde{b} = \tilde{a}$, the transition curve of the unimodal-bimodal transition tends to zero for large delay (see Fig. 5(b)). Consequently, as the delay becomes very large, the unimodal distribution exists only for very small noise amplitudes Q . In other words, for very large time delays the Hongler model is very sensitive to small noise intensities and the transition from the unimodal to the bimodal distribution occurs at very small critical noise amplitudes. In the case $\tilde{a} > |\tilde{b}|$, the transition curve tends to a constant as the time delay becomes large (see Fig. 5(c)). For $\tau \rightarrow \infty$ we obtain noise-induced transitions to bistability at a delay-independent critical noise amplitude $Q = 2\omega/c$.

Insert Figure 5 about here

4.3.2. Model with a noise amplitude of the form $1 - x^2$

Next, we consider a model that exhibits a noise amplitude proportional to $1 - x^2$. More precisely, we assume now that we have

$$\frac{d}{dt}X(t) = h(X, X(t - \tau)) + \sqrt{\tilde{Q}}(1 - X^2)\Gamma(t), \quad (39)$$

with $X \in [-1, 1]$. We require that for $\tilde{Q} = 0$ the drift force results in a unique stable fixed point at $x = 0$. A reducible model of the form Eq. (39) satisfying this requirement

is given by

$$\begin{aligned} \frac{d}{dt}X(t) = & -\tilde{a}(1-X^2)\operatorname{arctanh}(X) - \tilde{b}(1-X^2)\operatorname{arctanh}(X(t-\tau)) \\ & + \sqrt{\tilde{Q}}(1-X^2)\Gamma(t), \end{aligned} \quad (40)$$

with $\tilde{a}, \tilde{b} \in \mathbb{R}$. The appropriate variable transformation is given by $Y = \operatorname{arctanh}(X)$ and maps Eq. (40) to Eq. (2) with $a = \tilde{a}$, $b = \tilde{b}$ and $Q = \tilde{Q}$. From Eq. (24) it follows that the stationary distribution reads

$$P_{\text{st}}(x) = \frac{1}{\sqrt{2\pi K(\tau)}} \exp \left\{ -\frac{\operatorname{arctanh}^2(x)}{2K(\tau)} \right\} \frac{1}{1-x^2} \quad (41)$$

and exits for $\tilde{b} \geq |\tilde{a}|$ with $\tilde{a} \neq -\tilde{b}$ and $\tau < \tau_c$ and for $\tilde{a} > |\tilde{b}|$.

Insert Figure 6 about here

Let us discuss now the transition to bistability. Let x_e be the extremum of $P_{\text{st}}(x)$. Then x_e is a solution of

$$2x_e - \frac{\operatorname{arctanh}(x_e)}{K(\tau)} = 0. \quad (42)$$

Here $x_e \neq \{-1, 1\}$ and we suppose that $K(\tau) < \infty$. Obviously, the stationary distribution can have up to three extrema: Eq. (42) always has a trivial solution $x = 0$ and there might be a pair of nonzero solutions $-x_e$ and x_e . It can be easily seen that for $x_e \neq 0$, Eq. (42) can be written as $2K(\tau) = (1/x_e)\operatorname{arctanh}(x_e)$. It immediately follows that $K(\tau) > 1/2$. Therefore, $P_{\text{st}}(x)$ has the extrema at x_e and $-x_e$ when $K(\tau) > 1/2$ (see Fig. 6(b)). In contrast, the zero is the only maximum of $P_{\text{st}}(x)$ when $K(\tau) < 1/2$ (see Fig. 6(a)). From this fact we can summaries the qualitative different dynamical regimes in terms of the $\tau - Q$ parameter space as shown in Fig. 7. Note that again it is useful to distinguish between the cases $\tilde{b} > |\tilde{a}|$, $\tilde{a} = \tilde{b}$, $\tilde{a} > |\tilde{b}|$.

Insert Figure 7 about here

5. Conclusions

In this study, we derived a condition for which nonlinear time-delayed systems with multiplicative noise sources can be classified as reducible systems. More precisely,

we showed that when drift and diffusion functions satisfy a certain relationship then nonlinear SDDEs and DFPEs composed of these drift and diffusion functions can be transformed into linear SDDEs and DFPEs by means of particular variable transformations. In addition, we found that for such nonlinear but reducible SDDEs and DFPEs, analytical expressions for stationary distributions can be obtained. Moreover, we showed that the aforementioned variable transformations allow us to determine the parameter regions in which stationary distributions of reducible time-delayed stochastic systems exist.

In the context of dissipation-fluctuation relations, we studied the balance relation $\langle h \rangle = -\langle \xi \rangle$ that relates the drift h to an appropriately defined total fluctuating force ξ . We demonstrated that this balance relation becomes $\langle h \rangle = \langle \xi \rangle = 0$ for reducible systems provided that these reducible systems are studied in terms of transformed variables. In particular, we obtained an analytical expression for the average drift term $\langle h \rangle$ of a time-delayed stochastic Gompertz model. We showed how $\langle h \rangle$ depends on the time delay of the model and we found that $\langle h \rangle$ becomes constant for large time delays.

We demonstrated the power of our approach to nonlinear time-delayed systems with multiplicative noise sources by studying three reducible models in detail: a time-delayed Gompertz model with multiplicative noise, a time-delayed Hongler model, and a model involving a $1 - x^2$ noise amplitude and a time-delayed drift term. In particular, we derived the exact stationary distributions of these models.

As far as the Gompertz model is concerned, we derived the explicit form of the stationary distribution $P_{\text{st}}(x)$ involving the parameters $\tilde{a}, \tilde{b}, c, \tilde{Q}, \tau$. Since the Gompertz model is often found to fit data better than logistic and lognormal models [49], the exact stationary distribution $P_{\text{st}}(x)$ may be applied for statistical analysis. To this end, one can estimate the parameters $\tilde{a}, \tilde{b}, c, \tilde{Q}, \tau$ from experimental data by requiring that the experimentally observed distribution function $P_{\text{exp}}(x)$ fits $P_{\text{st}}(x)$ best in the sense that the Kullback-Leibler information [50] becomes minimal. In other words, we may choose $\tilde{a}, \tilde{b}, c, \tilde{Q}, \tau$ such that for these parameters $K = \int P_{\text{st}}(x) \ln(P_{\text{exp}}(x)/P_{\text{st}}(x)) dx$ assumes

a minimum.

In the case of Hongler model and the model with $1 - x^2$ noise amplitude, we found that the respective $\tau - Q$ parameter spaces can be split into three domains in which the systems exhibit qualitatively different stochastic behaviors. Transitions between unimodal and bimodal distributions as well as transitions between stationary and nonstationary states can occur when time delays or noise amplitudes are varied. In particular, the transitions to bistability depend both on the noise amplitudes and the time delays. For finite noise amplitudes the transition to the nonstationary case can only occur from the bimodal dynamical regime. That is, for finite noise amplitudes the unimodal distribution can not become unstable. There must be a transition to bistability before the transition to the nonstationary regime can occur. In this sense, the transition to non-stationarity can be regarded as a secondary transition. The reason for this behavior is that the variance $K(\tau)$ of the corresponding linear stochastic time-delayed system increases monotonically with the time delay (see Eq. (20)). The variance $K(\tau)$ can be regarded as a effective noise amplitude for the Hongler model and the model with $1 - x^2$ noise amplitude. Accordingly, if the transition to bistability occurs when the effective noise amplitude approaches a critical value K_c , whereas the transition to instability occurs when the effective noise amplitude tends to infinity. Since K increases monotonically with τ for any critical value K_c the variance K will first approach the critical value and subsequently tend to infinity. Only in the limit of vanishing noise (i.e. for $Q = 0$), there are triple points $(\tau, Q) = (\tau_c, 0)$ in the respective $\tau - Q$ parameter spaces of the Hongler model and the model with a $1 - x^2$ noise amplitude at which stable unimodal distributions, stable bimodal distributions and nonstationary states can co-exist (see Figures 5(a) and 7(a)).

Finally, we would like to point out that the exactly solvable nonlinear models discussed in our studies may be used as a testbed for numerical solvers of SDDEs [51] and perturbation theoretical approaches developed for SDDEs and DFPEs [52, 53].

Acknowledgments

This work is supported by the Thailand Research Fund with the grant from the Golden Jubilee Ph.D. Program according to the contact number PHD/0241/2545, 3. M. MU /45/B. 1.

6. References

- [1] R. Lang and K. Kobayashi, IEEE J. Quantum Electron. **16**, 347 (1980).
- [2] K. Ikeda and O. Akimoto, Phys. Rev. Lett. **48**, 617 (1982).
- [3] D. Lenstra, Optics Communications **81**, 209 (1991).
- [4] G. Giacomelli, R. Meucci, A. Politi, and F. T. Arecchi, Phys. Rev. Lett. **73**, 1099 (1994).
- [5] I. Fischer, O. Hess, W. Elsäßer, and E. Göbel, Phys. Rev. Lett. **73**, 2188 (1994).
- [6] M. Bestehorn, E. V. Grigorieva, H. Haken, and S. A. Kaschenko, Physica D **145**, 110 (2000).
- [7] C. Masoller, Phys. Rev. Lett. **88**, 034102 (2002).
- [8] K. Pyragas, Phys. Lett. A **170**, 421 (1992).
- [9] G. Stepan, *Retarded dynamical systems: stability and characteristic functions* (Longman Scientific & Technical, New York, 1989).
- [10] W. Wischert, A. Wunderlin, A. Pelster, M. Olivier, and J. Groslambert, Phys. Rev. E **49**, 203 (1994).
- [11] M. Schanz and A. Pelster, Phys. Rev. E **67**, 056205 (2003).
- [12] L. Larger, J. Goedgebuer, and T. Erneux, Phys. Rev. E **69**, 036210 (2004).
- [13] G. A. Bocharov and F. A. Rihan, J. Comput. Appl. Math. **125**, 183 (2000).
- [14] M. C. Mackey and L. Glass, Science **197**, 287 (1977).
- [15] A. Longtin, J. G. Milton, J. E. Bos, and M. C. Mackey, Phys. Rev. A **41**, 6992 (1990).
- [16] T. Ohira and J. G. Milton, Phys. Rev. E **52**, 3277 (1995).
- [17] J. L. Cabrera and J. G. Milton, Phys. Rev. Lett. **89**, 158702 (2002).
- [18] J. Sieber and B. Krauskopf, Physica D **197**, 332 (2004).
- [19] Y. Chen, M. Ding, and J. A. S. Kelso, Phys. Rev. Lett. **79**, 4501 (1997).
- [20] H. Hasegawa, Phys. Rev. E **70**, 021912 (2004).
- [21] H. Haken, *Brain dynamics* (Springer, Berlin, 2002).
- [22] A. Hutt, Phys. Rev. E **70**, 052902 (2004).
- [23] M. G. Rosenblum and A. S. Pikovsky, Phys. Rev. Lett. **92**, 114102 (2004).
- [24] H. Sompolinsky, D. Golomb, and D. Kleinfeld, Phys. Rev. A **43**, 6990 (1991).

- [25] V. K. Jirsa and M. Ding, *Phys. Rev. Lett.* **93**, 070602 (2004).
- [26] J. M. Cushing, *Integrodifferential equations and delay models in population dynamics* (Springer, Berlin, 1977).
- [27] F. Reif, *Fundamentals of statistical and thermal physics* (McGraw-Hill Book Company, New York, 1965).
- [28] W. Horsthemke and R. Lefever, *Noise-induced transitions* (Springer, Berlin, 1984).
- [29] L. M. Ricciardi, *Diffusion processes and related topics in biology* (Springer, Berlin, 1977).
- [30] L. Stark, F. W. Campbell, and J. Atwood, *Nature* **182**, 857 (1958).
- [31] S. Usui and L. Stark, *Biol. Cybern.* **45**, 13 (1982).
- [32] R. D. Driver, *Ordinary and delay differential equations — Applied mathematical sciences Vol. 20* (Springer, New York, 1977).
- [33] J. Hale, *Theory of functional differential equations* (Springer, Berlin, 1977).
- [34] R. Mankin, A. Ainsaar, and E. Reiter, *Phys. Rev. E* **60**, 1374 (1999).
- [35] H. Risken, *The Fokker-Planck equation — Methods of solution and applications* (Springer, Berlin, 1989).
- [36] U. Küchler and B. Mensch, *Stochastics and stochastic reports* **40**, 23 (1992).
- [37] A. A. Budini and M. O. Caceres, *J. Phys. A* **37**, 5959 (2004).
- [38] A. A. Budini and M. O. Caceres, *Phys. Rev. E* **70**, 046104 (2004).
- [39] T. D. Frank, *Phys. Rev. E* **69**, 061104 (2004).
- [40] C. Penland, *Physica D* **98**, 534 (1996).
- [41] R. Kubo, M. Toda, and N. Hashitsume, *Statistical Physics II* (Springer, Berlin, 1985).
- [42] U. Küchler and E. Platen, *Math. Comput. Simulat.* **54**, 189 (2000).
- [43] T. D. Frank and P. J. Beek, *Phys. Rev. E* **64**, 021917 (2001).
- [44] N. S. Goel, S. C. Maitra, and E. W. Montroll, *Rev. Mod. Phys.* **43**, 231 (1971).
- [45] M. Hongler, *Helv. Phys. Acta* **52**, 280 (1979).
- [46] C. R. Doering, *Phys. Rev. A* **34**, 2564 (1986).
- [47] C. R. Doering, *Phys. Lett. A* **122**, 133 (1987).
- [48] T. D. Frank, K. Patanarapeelert, and I. M. Tang, *Phys. Lett. A* **339**, 246 (2005).
- [49] R. Gutierrez, R. G. Sanchez, A. Nafidi, P. Roman, and F. Torres, *Cybernetics and systems* **36**, 203 (2005).
- [50] S. Kullback, *Information theory and statistics* (Dover Publications, New York, 1968).
- [51] C. T. H. Baker, *J. Comput. Appl. Math.* **125**, 309 (2000).
- [52] S. Guillouzic, I. L' Heureux, and A. Longtin, *Phys. Rev. E* **59**, 3970 (1999).
- [53] T. D. Frank, *Phys. Rev. E* **71**, 031106 (2005).

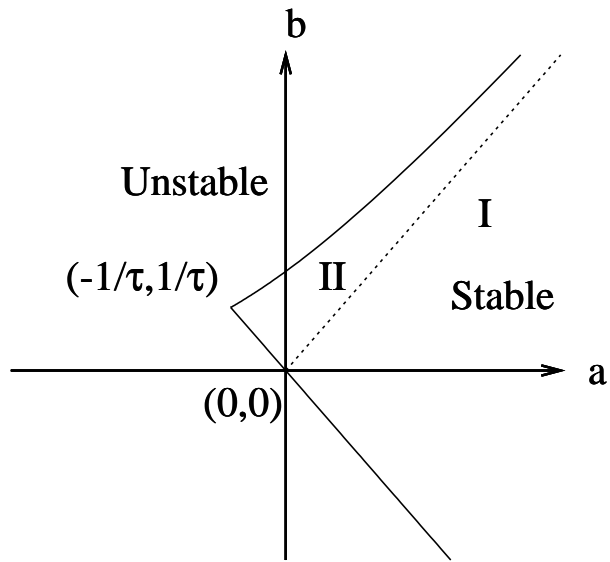


Figure 1. Parametric stability diagram for the linear SDDE (2). The stable region is defined by the intersection between two solid lines: one is the stationary bifurcation line $a = -b$ (lower line), the second is obtained from the parametric equations Eq. (17) (upper line). Subset I determines the stable region given by $a > |b|$ where the critical delay τ_c does not exist and subset II determines the stable region satisfy both $b > |a|$ and $\tau < \tau_c$.

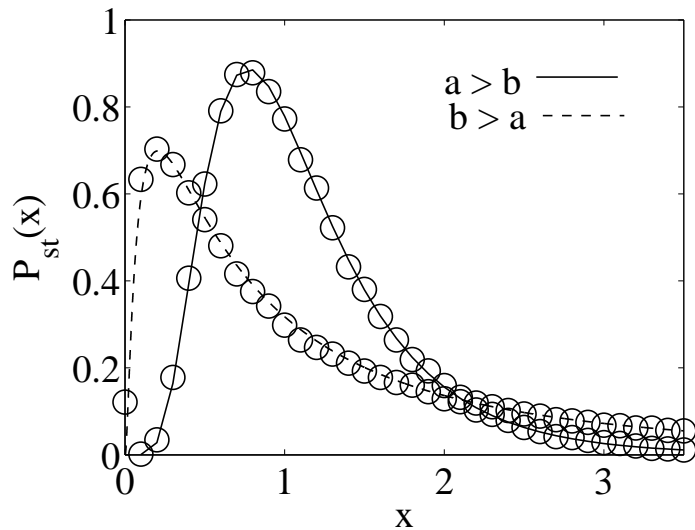


Figure 2. Stationary probability density of the Gompertz model (31) with parameters $Q = 1$, $c = 1$ and $\tau = 1$. Solid line: $(a, b) = (2, 1)$. Dashed line: $(a, b) = (1, 2)$. Circles represent the simulation results computed from $N = 10^5$ realizations and total integration time $T = 10^4$ with single time step $\Delta t = 10^{-2}$ and $x_0 = 0.1$ (see Sec. 4.1).

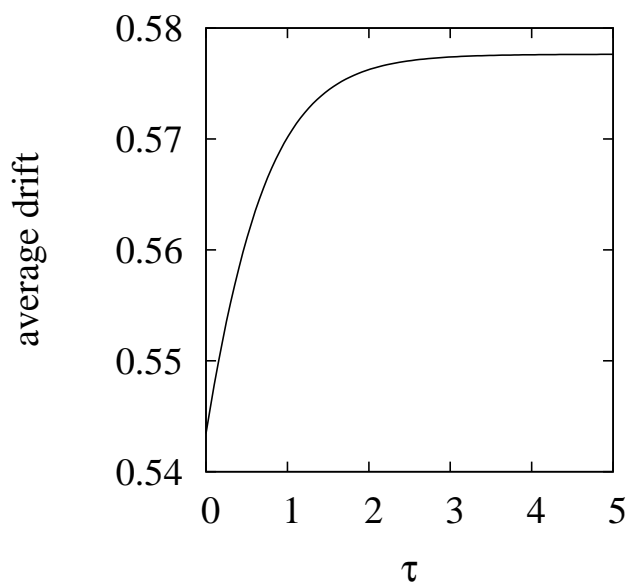


Figure 3. Average drift term $\langle h \rangle$ of the Gompertz model (31) as a function of time delay as computed from Eq. (35). The parameters are $Q = 1$, $c = 1$, $\tau = 1$, $b = 1$ and $a = 2$.

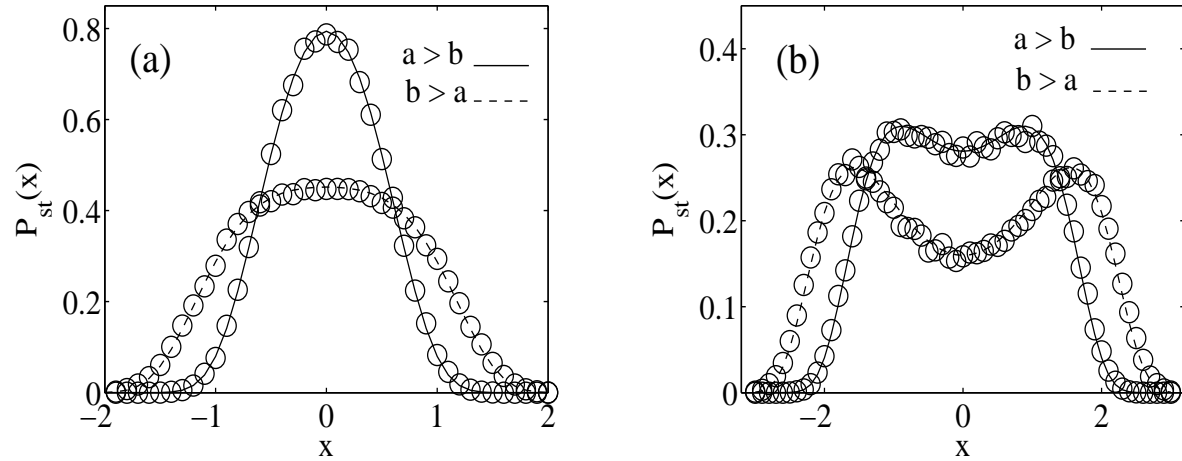


Figure 4. Noise- and delay-induced transitions to bistability demonstrated by the stationary probability density of the Hongler model (36). Panel a): Unimodal distribution with parameters $Q = 1$, $c = 1$ and $\tau = 0.8$. Solid line: $(a, b) = (2, 1)$. Dashed line: $(a, b) = (1, 2)$. Panel b): Bimodal distribution with parameters $Q = 8$, $c = 1$ and $\tau = 0.8$. Solid line: $(a, b) = (2, 1)$. Dashed line: $(a, b) = (1, 2)$. Circles represent the simulation results ($N = 10^5$, $T = 10^4$, $\Delta t = 10^{-2}$, $x_0 = 0.1$).

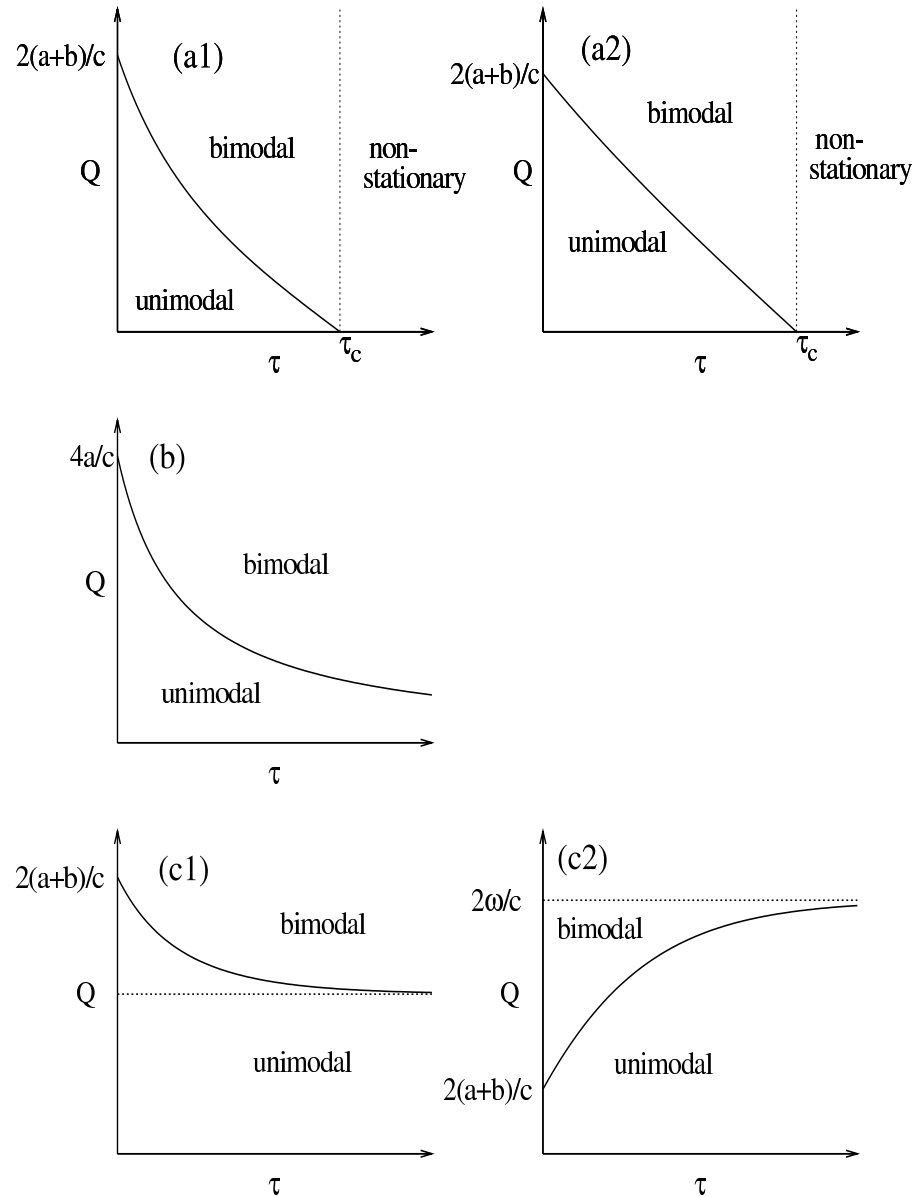


Figure 5. Generalized phase diagrams on the $\tau - Q$ plane for the Hongler model. Solid lines are plotted from $K(\tau) = 1/c^2$ and Eq. (19). Panel a1): $b > |a|$ with $a = 1$ and $b = 2$. Panel a2): $b > |a|$ with $a = -1$ and $b = 2$. Panel b): $a = b = 1$. Panel c1): $a > |b|$ with $a = 2$ and $b = 1$. Panel c2): $a > |b|$ with $a = 2$ and $b = -1$.

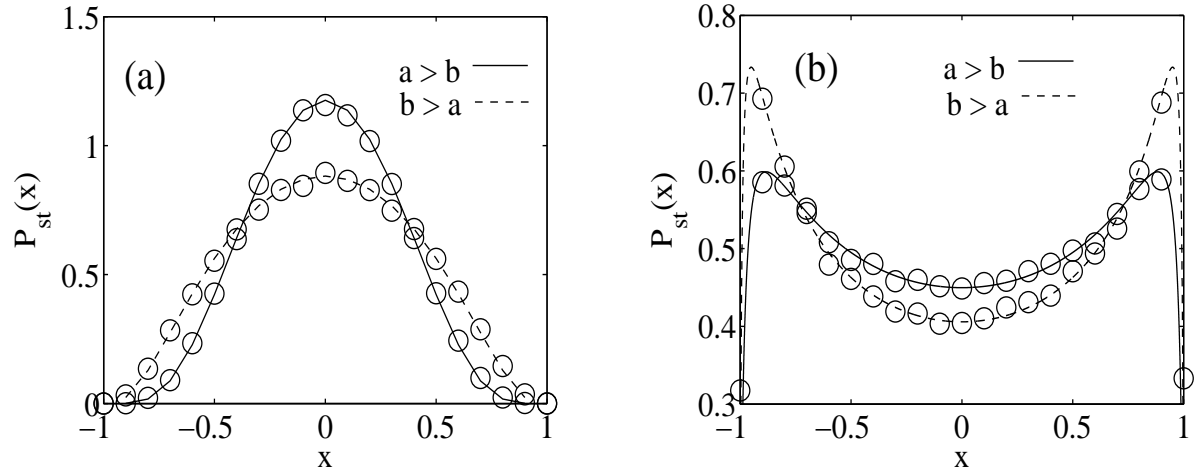


Figure 6. Noise- and delay-induced transitions to bistability demonstrated by the stationary probability density of the $1 - x^2$ noise model. Panel a): Unimodal distribution with parameters $Q = 0.5$ and $\tau = 0.5$. Solid line: $(a, b) = (2, 1)$. Dashed line: $(a, b) = (1, 2)$. Panel b): Bimodal distribution with parameters $Q = 4$ and $\tau = 0.2$. Solid line: $(a, b) = (2, 1)$. Dashed line: $(a, b) = (1, 2)$. Circles represent the simulation results ($N = 10^5$, $T = 10^4$, $\Delta t = 10^{-2}$, $x_0 = 0.1$).

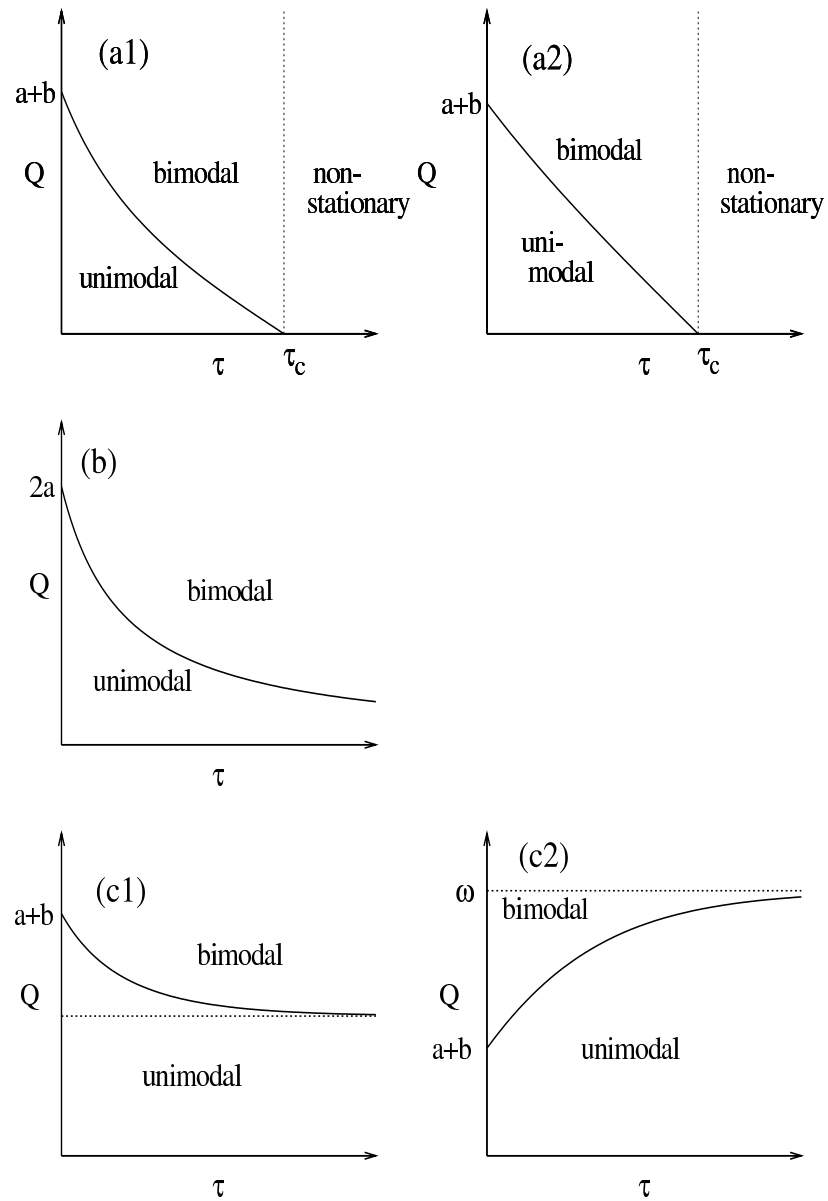


Figure 7. Phase diagrams on the $\tau - Q$ plane for $1 - x^2$ noise model. Solid lines are plotted from $K(\tau) = 1/2$ and Eq. (19). Panel a1): $b > |a|$ with $a = 1$ and $b = 2$. Panel a2): $b > |a|$ with $a = -1$ and $b = 2$. Panel b): $a = b = 1$. Panel c1): $a > |b|$ with $a = 2$ and $b = 1$. Panel c2): $a > |b|$ with $a = 2$ and $b = -1$.